JAERI-Tech
2000-022

THERMAL AND CHEMICAL ANALYSIS OF CARBON DIOXIDE REFORMING OF METHANE USING THE OUT-OF-PILE TEST FACILITY

March 2000

Ziyong HUANG*, Hirofumi OHASHI and Yoshiyuki INAGAKI

日本原子力研究所
Japan Atomic Energy Research Institute

編集兼発行　日本原子力研究所

JAERI-Tech 2000-022

Thermal and Chemical Analysis of Carbon Dioxide Reforming of Methane Using the Out-of-Pile Test Facility

Ziyong HUANG*, Hirofumi OHASHI and Yoshiyuki INAGAKI

Department of Advanced Nuclear Heat Technology
Oarai Research Establishment
Japan Atomic Energy Research Institute
Oarai-machi, Higashiibaraki-gun, Ibaraki-ken

(Received February 1, 2000)

In the Japan Atomic Energy Research Institute, a hydrogen production system is being designed to produce hydrogen by means of steam reforming of natural gas (its main composition is methane(CH_4)) using nuclear heat (10MW, 1178K) supplied by the High Temperature Engineering Test Reactor (HTTR). Prior to coupling of the steam reforming system with the HTTR, an out-of-pile demonstration test was planned to confirm safety, controllability and performance of the steam reforming system under simulated operational conditions of the prototype. The out-of-pile test facility simulates key components downstream to an intermediate heat exchanger of the HTTR hydrogen production system on a scale of 1: 30 and has a hydrogen production capacity of 110 Nm^3/h using an electric heater as a reactor substitute. The test facility is presently under construction.

Reforming of natural gas with carbon dioxide CO_2 (CO_2 reforming) using the out-of-pile test facility is also being considered. In recent years, catalytic reforming of natural gas with CO_2 to synthesis gas (CO and H_2) has been proposed as one of the most promising technologies for utilization of those two greenhouse gases. Numerical analysis on heat and mass balance has practical significance in CO_2 reforming when the steam reforming process is adopted in the out-of-pile test. Numerical analysis of CO_2 reforming and reforming of natural gas with CO_2 and steam (CO_2+H_2O reforming) have been carried out using the mathematical model. Results such as the methane conversion rate, product gas composition, and the components temperature distribution considering the effects of helium gas temperature, reforming pressure, molar ratio of process gases and so on have been obtained in the numerical analysis. Heat and mass balance of the out-of-pile test facility considering chemical reactions are evaluated well. The methane conversation rates are about 0.36 and 0.35 which correspond to the equilibrium at 1085 and 1100K for CO_2 reforming and CO_2+H_2O reforming at each given standard condition (He temperature is 1153K), respectively. The results show that tests of the CO_2 reforming and CO_2+H_2O reforming can be carried out in the out-of-pile test facility without reconstruction of the facility.

Keywords: HTGR, HTTR, Nuclear Heat Utilization, Hydrogen Production, Out-of-Pile Test, Reforming of Natural Gas, Exothermic and Endothermic Reactions, Methane, Carbon Dioxide, Synthesis Gas

---

*Institute of Nuclear Energy Technology, Tsinghua University

JAERI-Tech 2000-022

炉外技術開発試験装置における天然ガスの二酸化炭素改質反応の熱化学解析

日本原子力研究所大洗研究所核熱利用研究部
黄　志勇*・大橋　弘史・稲垣　嘉之

（2000年2月1日受理）

日本原子力研究所では、高温ガス炉、高温工学試験研究炉（HTTR）から供給される核熱（10MW、1178K）を利用し、天然ガス（主成分：メタン）の水蒸気改質反応により水素を製造するHTTR水素製造システムを計画している。そこで、HTTRとの接続の前に、安全性、制御性および水蒸気改質システムの性能を明らかにすることを目的として、通電式加熱器を用いて中間熱交換器以降を模擬した水素製造量1/30スケール（110Nm^3/h）の炉外技術開発試験を計画し、試験装置の建設を行っている。

一酸化炭素と水素から成る合成ガスを製造する天然ガスの二酸化炭素改質反応（CO_2改質）は、近年、温室ガスの低減技術として期待されており、炉外技術開発試験装置における試験の実施が検討されている。しかし、水蒸気改質のために設計された炉外技術開発試験装置を用いてCO_2改質を行うにあたり、熱・物質収支計算による改質器性能の事前解析が必要である。そこで、本研究では、CO_2改質および二酸化炭素と水蒸気を同時に供給し、CO_2改質と水蒸気改質を同時に行う場合（CO_2+H_2O 改質）について、数値解析による改質器性能解析を行い、圧力、温度、原料ガス組成等の転化率および生成ガス組成に対する影響を明らかにした。数値解析の結果、設定した定格運転時（改質器入口 He 温度 1153K）のCO_2改質およびCO_2+H_2O改質のメタン転化率は、各々1085、1100Kにおける平衡転化率と等しい0.36、0.35であった。これらの結果より、炉外技術開発試験装置がCO_2改質およびCO_2+H_2O 改質にも使用可能であることをが明らかにした。

大洗研究所：〒311-1394　茨城県東茨城郡大洗町成田町新堀3607
*清華大学核能技術設計研究院

Contents

目次

1. Introduction

1.1 Nuclear Power and the Environment

In 1998, some 434 nuclear reactors operating in 31 countries provided over 16% of global electricity and accounted for the avoidance of about 8% of global carbon emissions. Accumulated operating experience for nuclear power reactors has reached over 9,000 reactor-years. Improved safety and reliability of nuclear power plants over the past decade has been evident.

Concern about global warming and climate change has led industrialized countries to agree to lower their emissions of man-made greenhouse gases in accordance with the targets specified in the Kyoto Protocol. Other countries have announced similar voluntary commitments. Energy produced from fossil fuels accounts for about half of man-made greenhouse gases emissions. While there are many hopes for 'clean' energy sources, the fact is that except for nuclear or hydropower, there are not yet any other economically viable, minimal- greenhouse gases -emission options for large scale power generation.

The global challenge is to develop strategies that foster a sustainable energy future that will be less dependent on fossil sources. The energy choices for the future need to take account of targets and timetables for reducing carbon dioxide emissions. Nuclear power will grow as a key part of energy strategies for sustainable development, together with an increased use of renewable sources, improved fossil fuel conversion and a greater efficiency throughout the energy system.

Consumption of a huge amount of fossil fuels has further aggravated global warming. In order to relieve the global warming conditions (that is the need to reduce carbon dioxide (CO_2) emissions to the atmosphere) new energy resources and technologies need to be developed.

Hydrogen (H_2) is a clean fuel in the sense that no CO_2 is emitted by its use. Methods for hydrogen production are necessary that are both economic as well as environmentally acceptably- i.e. without anthropogenic release of CO_2 to the atmosphere.

With the current abundance of natural gas (of which the main element is methane (CH_4)) there is continuing interest in the conversion of CH_4 to more useful products such as hydrogen and methanol.

1.2 Hydrogen Energy

1.2.1 Hydrogen Energy

Most industrial, residential, and commercial fuel requirements can be met hydrogen using existing technology. The expectation is that this technology will continue to improve. The hydrogen-electrical conversion could be accomplished in fuel cells or in gas turbines. Hydrogen has many attractive features as the principal synthetic fuel. For example: It can be manufactured by natural gas reforming, the decomposition of water; all of the future primary energy sources are suitable for hydrogen production; When combined with air the only by-products are water vapor and oxides of nitrogen (the NO_x can be controlled and suppressed by selection of combustion conditions); The heat of combustion per unit weight is larger than for any other practical fuel; It can be transported cheaply by pipeline; It is an excellent general purpose fuel, probably better than any other practical fuel; Spills dissipate rapidly under conditions of good ventilation; And, it is less toxic than other fuels. Syngas of H_2 and carbon monoxide (CO) produced by methane reforming have many industrial process applications:

(1) Coal gasification $C + 2H_2 = CH_4$ (1.1)
(2) Direct usage in steel production $Fe_2O_3 + 3H_2 = 2Fe + 3H_2O$ (1.2)
$Fe_2O_3 + 3\ CO = 2Fe + 3\ CO_2$ (1.3)
(3) To produce ammonia $N_2 + 3H_2 = 2NH_3$ (1.4)
(4) To produce methanol $CO + 2H_2 = CH_3OH$ (1.5)
(5) Chemical heat pipe $CO + 3H_2 = CH_4 + H_2O$ (1.6)
(6) To product hydrocarbon $6CO + 13H_2 = C_6H_{14} + 6H_2O$ (1.7)

1.2.2 Methane Reforming with Steam

The major part of the world's hydrogen production is accomplished by reforming natural gas by using steam reforming (Eq.(1.8)), followed by a water-gas shift reaction (Eq.(1.9)). Production of hydrogen by conventional technology such as steam reforming combined with CO_2 separation and sequestration, is not a new concept.

$$CH_4 + H_2O\ (g) = CO + 3H_2 \qquad -206\ \text{kJ/mol} \tag{1.8}$$

$$CO + H_2O\ (g) = CO_2 + H_2 \qquad +41.2\ \text{kJ/mol} \tag{1.9}$$

Reactions (1.8) is endothermic whereas reaction (1.9) is exothermic. In order to supply the large endothermic reaction heat and to maintain that high temperature around 1200K, additional heat is supplied through fossil fuel combustion. Since, the conversion of methane is limited by thermodynamic equilibria, high temperatures and low pressures aid this conversion process. It is noteworthy that only half of the hydrogen produced originates from the hydrocarbon. The energy used for the endothermic reaction such as steam reforming can be supplied by nuclear energy or solar energy, non fossil fuel energy etc. The produced CO and H_2 can be transported to another place demanding energy. There, at low temperature, it is all right to do the methanation ($CO + 3H_2 \rightarrow CH_4 + H_2O$), the purpose of utilization of heat can be achieved. This is the called EVA-ADAM process operated at the KFA, Germany (1).

1.2.3 Methane Reforming with Carbon Dioxide (2-8)

CH_4 and CO_2 which often co-exist in nature constitute valuable potential resources both for the storage of thermal energy and the conventional production of synthesis gas. The reforming of CH_4 with CO_2 (CO_2 reforming) is expressed as the following equation

$$CH_4 + CO_2 = 2CO + 2H_2 \quad -248\ \text{kJ/mol} \tag{1.10}$$

There are also the environmental benefits of reducing global greenhouse gas effects by CO_2 reuse as a renewable resource. There are some applications where CO_2 reforming will need to be conducted in the absence of steam reforming, such as:

- Efficient production of dimethyl ether, both as an intermediate for the production of synthetic gasoline and as a raw material for the production of a range of industrially important ethers and esters.
- Thermochemical heat pipe applications for the recovery, storage and transmission of solar and other renewable energy sources. This concept involves using a high temperature energy sources to supply the heat for a strongly endothermic reaction (CO_2 reforming). The reaction products (CO and H_2) can be then stored or transported to a separate site and subsequently used for the reverse reaction ($2CO + 2H_2 \rightarrow CH_4 + CO_2$), thereby releasing the stored chemical energy. The products of the reverse reaction are then sent back to the endothermic reactor to complete the closed loop cycle. Therefore, in certain potential application such as the above, CO_2 reforming has unique advantages over steam reforming, and is likely to become an increasingly important industrial process in the foreseeable future. However, CO_2 reforming is highly endothermic (ΔH=260 kJ/mol, at 1073K) and hence a highly energy intensive process. Further, it yields synthesis gas with a H_2/CO ratio of less than 1.0 which is not suitable for Fischer-Tropsch synthesis processes (which requires H_2/CO ratio is between 1.0 and 2.0) and also involves rapid coke deposition, particularly on a nickel catalyst. It is necessary to avoid feeding reactants at a lower temperature than at the rated temperature and the limiting temperature. Because catalyst degradation due to carbon deposition (T=950K), and catalyst degradation due to steam condensation (T=600K), causes flow choke.

Recently, new catalysts are being developed to prevent the production of carbon. A catalyst is defined as a chemical substance, which increases the rate of a chemical reaction without itself being consumed in the reaction. Very often, the catalytic process occurs at the surface of a solid particle that is in contact with the gaseous mixture. This is called heterogeneous catalysis. Catalyst that has commercial applications should have good comprehensive performances that are high activity, resistance for carbon deposition, low temperature reducibility, as well as having high strength and stability. However, the conventional Ni-based steam reforming catalysts are likely to coke severely if they are used for CO_2 reforming alone. The catalysts are easily deactivated by carbon deposition, which is a serious problem. The catalytic activity and the extent of coking changes significantly with the use of different supports. This may be due to the activation of CH_4 or CO_2 on supports themselves working bifunctionally with metal components. Deactivation of supported metal catalyst by carbon formation is a very serious problem. Its causes are generally threefold (1)fouling of the metal surface, (2)blockage of catalyst pores and voids and (3) break-up of the catalyst support material. There is thus a need to develop catalysts especially for this reaction. This currently is of considerable worldwide research interest. Therefore, one of the major challenges in the commercialization of the CO_2 reforming reaction is to develop catalysts, which can efficiently enhance chemical reactions without any net formation of carbon. Group Ⅷ metals in their elemental (reduced) forms, especially, Ni, Ru, Rh, Pd, Ir, and Pt are active catalysts for the CO_2 reforming and appear to constitute effective catalytic components. These elements are identified as the best catalytic potential for the CO_2 reforming reaction when put on suitable supports. Catalysts commonly used for CO_2 reforming are as follows: Ni-La_2O_3-Ru, Ni-Ce_2O_3-Pt, Ni-MgO, Ni-SiO_2, NiO-CaO, Rh-Al_2O_3, Ru-Eu_2O_3, Ir-Eu_2O_3 etc. Activity comparison of catalysts is listed below:

SiO_2 support: Ru> Rh> Ni> Pt>> Pd;

or Ni> Ru> Rh> Pt> Pd >> Co.

MgO support: Ru> Rh> Ni> Pd> Pt.

Al_2O_3 support: Ru> Pd> Rh> Pt> Ir;

or Rh> Pd> Pt>> Ru;

Ni> Co>>Fe.

Regarding the Rh catalyst, the activity increases on support as below:

$$Al_2O_3 > TiO_2 > SiO_2$$

Ni-based three-component catalysts such as Ni-La_2O_3-Ru or Ni-Ce_2O_3-Pt supported on alumina wash-coated ceramic fiber in a plate shape were very suitable for the reforming of methane with H_2O, CO_2, and H_2O+CO_2. It should be pointed out that sulphur poisoning also cause catalyst deactivation. Normally, sulphur will be present in natural gas, which can be purified effectively to a tolerable content proceeding the steam reforming. Because sulphur adsorbs so strongly on nickel, its presence on a catalyst surface usually causes substantial loss of activity in the steam reforming. The alumina-supported Rh catalyst is founded to have the highest activity (with higher methane conversion) compared with Pt or Pd. Thus, Rh appears intrinsically to be the most suitable catalyst. A prominent enhancement in the methane reforming reaction with CO_2 and H_2O has been observed by modifying the Ni-CeO_2-Pt catalyst with a small amount (0.2 wt.-%) of Rh. Some kinds of catalyst, such as Ni and Rh, will be examined according to the scheduled in out-of-pile test.

1.2.4 Methane Reforming with Carbon Dioxide and Steam

Although there has yet been no large scale commercial applications of CO_2 reforming, it has been used in conjunction with the widely applied steam reforming process, with the aim of producing synthesis gases with the required $H_2/(CO+CO_2)$ ratios to meet specific end-use requirements such as methanol production. The reforming of CH_4 with CO_2 and H_2O (CO_2+H_2O reforming) consists of the elementary reactions Eq.(1.8) and (1.10) If the molar ratio of the reactant gas, $CH_4 : CO_2 : H_2O$ is 3 : 1 : 2, the overall reaction equation can be expressed as follows

$$3CH_4 + CO_2 + 2H_2O = 4CO + 8H_2 \tag{1.11}$$

The molar ratio of synthesis gas products of CO to H_2 is 4 : 8 (i.e. 1:2), which can be used to produce exactly 1 mole of methanol as an end product through the Eq.(1.5).

1.3 HTTR Hydrogen Production System (9)

Nuclear energy has the advantage of being able to supply energy in large quantities for a long time and almost free from the emission of greenhouse gases. Therefore, it continues to play an important role in the Japan Atomic Energy Research Institute (JAERI) as they conduct R&D in advanced fields of nuclear energies, as well as in the improving safety and the reliability of nuclear energy systems. JAERI is also promote advanced and basic research in conjunction with nuclear energy research for progress in the utilization of nuclear energy. Nuclear reactors can satisfy a large amount of energy demands without significant CO_2 emissions, especially, with High-Temperature Gas-cooled Reactor (HTGR). These provide a high-temperature nuclear heat source with high thermal efficiency, that are applicable to both electric and non-electric fields. JAERI has been constructing a 30MW HTGR with a reactor outlet coolant temperature of 1223K, named HTTR. The first criticality of the HTTR was attained on the 10th of November 1998. Reactor performance and safety demonstration tests of HTTR will be carried out for several years, and after that, a high-temperature nuclear heat utilization system will be coupled with the HTTR. A hydrogen production system using the reforming of natural gas with steam is to be the first heat utilization system of the HTTR, since technology matured in fossil-fired plants. Technical solutions demonstrated by the coupling will contribute to all other hydrogen production systems. Also, a hydrogen production system is considered as one of the leading nuclear heat utilization systems in the non-electric field because hydrogen has superior characteristics as an energy carrier and its demand is expected to increase in the future.

1.4 Feasibility of Methane Reforming with Carbon Dioxide in Out-of-Pile Test Facility

Prior to the coupling of the steam reforming system with the HTTR, an out-of-pile test is planned to confirm safety, controllability and performance of the steam reforming system under simulated operational conditions (10, 11). After successful demonstration of the steam reforming in the out-of-pile test facility, the CO_2 reforming is considered as the next test because the steam reforming system is exchangeable with the CO_2 reforming system.

For steam reforming, the enthalpy for the reaction ΔH_1= -206kJ/mol;

For CO_2 reforming, the enthalpy for the reaction ΔH_2= -248kJ/mol;

The chemical heat needed in the process is almost the same. ΔH_2 is 42 kJ/mol higher than ΔH_1.

For a complete chemical and thermal process, there is an example, at Pressure $P_1=P_2=4.6MPa$,

From water of 20℃ to steam of 450℃, the heat needed is: Q_1=-68 kJ/mol;

From CO_2 of 20℃ to CO_2 of 450℃, the heat needed is: Q_2=-20 kJ/mol;

So the total quantity of heat needed is:

$Q_{total1} = \Delta E_1 + Q_1 = (-206) + (-68) = -274$ kJ/mol;

$Q_{total2} = \Delta E_2 + Q_2 = (-248) + (-20) = -268$ kJ/mol;

The difference between Q_{total1} and Q_{total2} is just 6kJ/mol. Therefore, the design, equipment etc. of steam reforming system might be able to use again. When CO_2 is added to the system of steam reforming, the ratio of CO to H_2 in product gas is adjustable. For example, if the molar ratio between CO and H_2 is 1: 2, the formation of methanol (expressed by Eq.(1.5)) can be conducted. And if the molar ratio between CO and H_2 is 1: 1, acetic acid forming can be conducted.

$$2CO + 2H_2 = CH_3COOH \qquad (1.12)$$

Methanol and acetic acid can be stored and transported as fossil fuel. It should seriously be considered as a future energy source.

In this study, numerical analysis of CO_2 reforming and CO_2+H_2O reforming were carried out using the numerical model. Results such as the methane conversion ratio, product gas composition and the temperature distribution of components effected by the helium gas temperature, reforming pressure, molar ratio of process gases and so on have been obtained in the numerical analysis.

2. Out-of-Pile Test Facility

The main objectives of the out-of-pile test are the investigation of hydrogen production performance and transient behaviors of the hydrogen production system, and the establishment of operation and control technologies well-matched with the reactor operation, as well as the design verification of the performance of high-temperature components such as a reformer and steam generator. The simplified schematic diagram of the out-of-pile test facility (1) is shown in Fig.2.1. The facility simulates key components downstream from the intermediate heat exchanger of the HTTR hydrogen production system on a scale of 1 to 30 and has a hydrogen production capacity of 110 Nm^3/h using an electric heater as a reactor substitute. Design specifications of the HTTR hydrogen production system and out-of-pile test facility are listed in Table2.1.

The schematic diagram of a reformer is shown in Fig.2.2. The reformer has one bayonet-type catalyst tube made of Alloy 800H whose dimensions (such as diameter and length) are approximately the same as those of the catalyst tube of the HTTR hydrogen production system. The reformer of the HTTR hydrogen production system has 30 bayonet-type catalyst tube made of Hastelloy XR. Process gas (CH_4 and H_2O) flows in the catalyst tube at an inlet temperature of 723K and helium gas flows in a channel between the catalyst and guide tubes at an inlet temperature of 1153K.

In the fossil-fired plant, the process gas receives heat from combustion of about 1473K by radiation, and the heat flux at the outer surface of the catalyst tube reaches 70,000-87,000 W/m^2. In order to achieve the same heat flux as that of the fossil-fired plant, it is very important to promote the heat transfer of helium gas by forced convection because the temperature of helium gas, that is, the temperature of the heat source is too low compared with that of the fossil-fired plant. So, disc-type fins, 2mm in height, 1mm in width and 3mm in pitch, are arranged around the outer surface of the catalyst tube in the test facility in order to increase a heat transfer coefficient of helium gas by 2.7 times, 2150W/m^{2}K with the fins, and a heat transfer area by 2.3 times larger than those of smooth surface, respectively. As the result, the heat transfer performance of the catalyst tube in the test facility becomes competitive to that of the fossil-fired plant.

Table 2.1 Design specification of HTTR hydrogen production system and out-of-pile test facility

Item		HTTR	Out-of-Pile
He	Temperature at steam reformer (inlet / outlet)	1153K (= 880°C) / 873K (= 600°C)	1153K (= 880°C) / 923K (= 650°C)
	Exit pressure at steam reformer	4.0MPa	
	Feed flow rate	2.43kg/s	0.091kg/s
Process gas	Temperature at steam reformer (inlet / outlet)	723K (= 450°C) / 873K (= 600°C)	
	Inlet pressure at steam reformer	4.3MPa	
	Natural gas feed flow rate	0.36kg/s (= 81kmol/h)	0.012kg/s (= 2.7kmol/h)
	H_2O / CH_4 (molar ratio)	3.5	2 ~ 4
Hydrogen product		3800Nm^3/h	110Nm^3/h
Heat source		Reactor (10MW)	Electric heater (380kW)

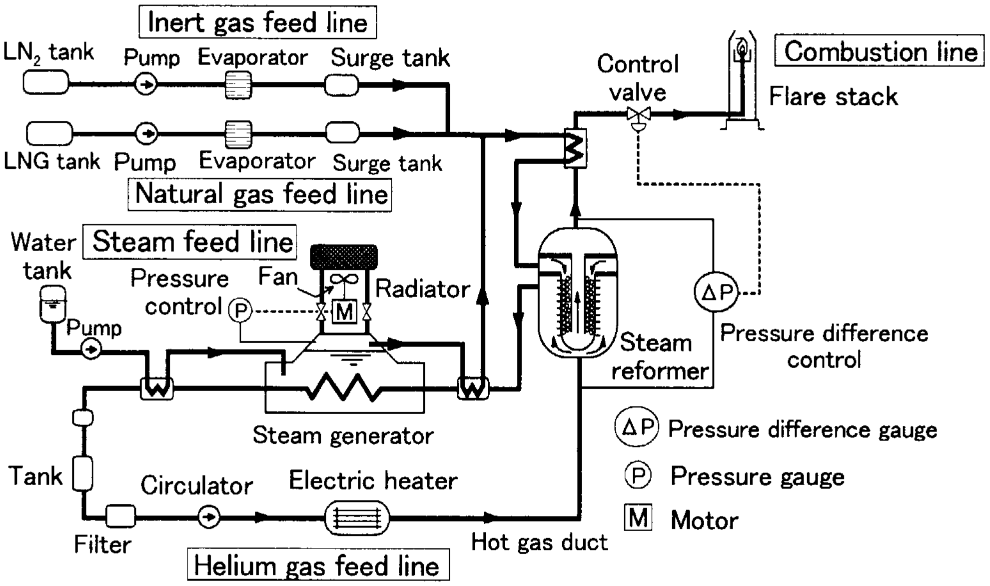

Fig 2.1 Simplified schematic diagram of out-of-pile test facility

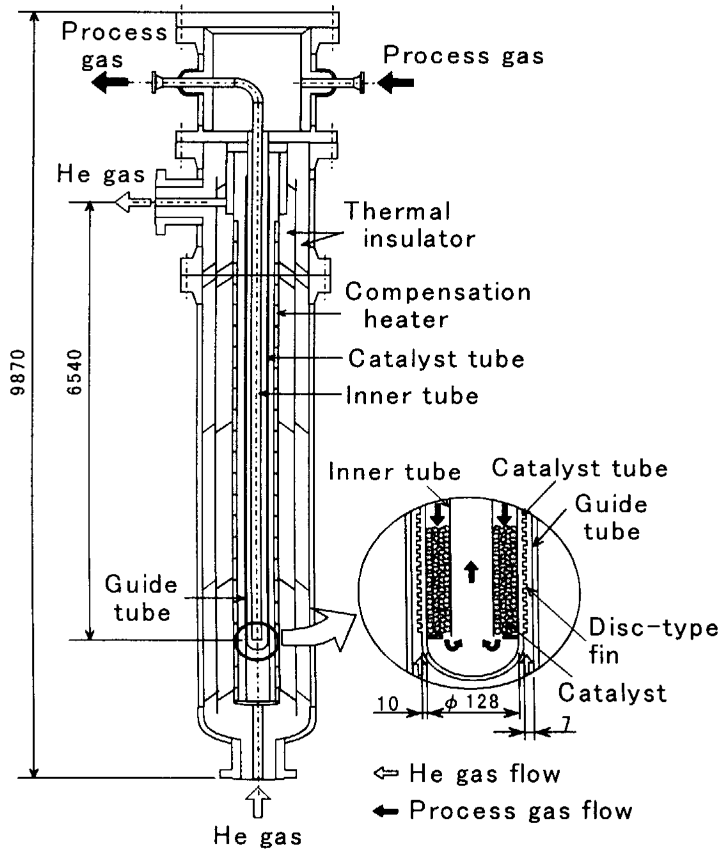

Fig 2.2 Schematic view of steam reformer

3. Numerical Model

3.1 Governing Equations of Gas Phase Flow

Assuming one-dimensional compressible fluid, gas flow behavior in the pipe, which is connected with the reformer, is analyzed using following equations:

Mass equation: $$\frac{\partial \rho}{\partial t} + \frac{\partial(\rho \cdot u)}{\partial x} = 0 \qquad (3.1)$$

Momentum equation: $$\frac{\partial(\rho \cdot u)}{\partial t} + u\,\frac{\partial(\rho \cdot u)}{\partial x} = -\frac{\partial P}{\partial x} - \rho \cdot F - \rho \cdot g \cdot \sin\theta \qquad (3.2)$$

Energy equation: $$\frac{\partial\left\{\rho\left(e + \frac{u^2}{2}\right)\right\}}{\partial t} + \frac{\partial\left\{\rho \cdot u\left(h + \frac{u^2}{2}\right)\right\}}{\partial x} = Q_w - \rho \cdot u \cdot g \cdot \sin\theta \qquad (3.3)$$

Gas state equation: $$\rho = \frac{P}{R \cdot T \cdot \sum(m_i / M_i)} \qquad (3.4)$$

Where $$F = \frac{1}{2}\left(\frac{f}{D} + \frac{\varsigma}{L}\right) \cdot u^2 \qquad (3.5)$$

$$e = \sum m_i \cdot C_{v,i} \cdot T \qquad (3.6)$$

$$h = \sum m_i \cdot C_{P,i} \cdot T = e + \frac{P}{\rho} \qquad (3.7)$$

3.2 Heat and Mass Balance of Reformer

3.2.1 Heat Balance Equations

Schematic diagram of a reformer is shown in Fig.3.1. Heat balance equations for each cell are as follows;

Product gas $$C_{1,j} \cdot W_{1,j}\,\frac{dT_{1,j}}{dt} = A^i_{2,j} \cdot \alpha^i_{2,j} \cdot \left(T_{2,j} - T_{1,j}\right) + C_{1,j} \cdot G_{1,j}\left(\theta_{1,j} - \theta_{1,j+1}\right) \qquad (3.8)$$

Inner tube $$C_{2,j} \cdot W_{2,j}\,\frac{dT_{2,j}}{dt} = A^0_{2,j} \cdot \alpha^0_{2,j}\left(T_{3,j} - T_{2,j}\right) + A^i_{2,j} \cdot \alpha^i_{2,j}\left(T_{1,j} - T_{2,j}\right) \qquad (3.9)$$

Reactant gas

$$\begin{aligned} C_{3,j} \cdot W_{3,j}\,\frac{dT_{3,j}}{dt} &= A^i_{4,j} \cdot \alpha^i_{4,j}\left(T_{4,j} - T_{3,j}\right) + A^0_{2,j} \cdot \alpha^0_{2,j}\left(T_{2,j} - T_{3,j}\right) \\ &\quad + A_{c,j} \cdot \alpha_{c,j}\left(T_{c,j} - T_{3,j}\right) + C_{3,j} \cdot G_{3,j}\left(\theta_{2,j+1} - \theta_{2,j}\right) - Q_{3,j} \end{aligned} \qquad (3.10)$$

where $Q_{3,j} = f(\theta_{2,j}, component_j) - f(\theta_{2,j+1}, component_{j+1})$

Catalyst particle $$C_{c,j} \cdot W_{c,j} \frac{dT_{c,j}}{dt} = A_{c,j} \cdot \alpha_{c,j} \left(T_{3,j} - T_{c,j} \right) \tag{3.11}$$

Outer pipe $$C_{4,j} \cdot W_{4,j} \frac{dT_{4,j}}{dt} = A^0_{4,j} \cdot \alpha^0_{4,j} \left(T_{5,j} - T_{4,j} \right) + A^i_{4,j} \cdot \alpha^i_{4,j} \left(T_{3,j} - T_{4,j} \right) \tag{3.12}$$

Helium $$\begin{aligned} C_{5,j} \cdot W_{5,j} \frac{dT_{5,j}}{dt} &= A_{r,j} \cdot \alpha_{r,j} \left(TI_{1,j} - T_{5,j} \right) + A^0_{4,j} \cdot \alpha^0_{4,j} \left(T_{4,j} - T_{5,j} \right) \\ &\quad + C_{5,j} \cdot G_{5,j} \left(\theta_{3,j} - \theta_{3,j+1} \right) \end{aligned} \tag{3.13}$$

Heat insulating material

(inner side) $$\frac{\partial^2 TI}{\partial s^2} + \frac{1}{s} \frac{\partial TI}{\partial s} = \frac{1}{a_1} \frac{\partial TI}{\partial t} \tag{3.14}$$

(outer side) $$\frac{\partial^2 TI}{\partial s^2} + \frac{1}{s} \frac{\partial TI}{\partial s} = \frac{1}{a_2} \frac{\partial TI}{\partial t} \tag{3.15}$$

Boundary conditions $$- \lambda_1 \left. \frac{\partial TI}{\partial s} \right|_{s=s_1} = \alpha_{r,j} \left(T_{5,j} - TI_{1,j} \right) \tag{3.16}$$

$$- \lambda_1 \left. \frac{\partial TI}{\partial s} \right|_{s=sN1} = - \lambda_2 \left. \frac{\partial TI}{\partial s} \right|_{s=sN1} \tag{3.17}$$

$$- \lambda_2 \left. \frac{\partial TI}{\partial s} \right|_{s=sN2} = \alpha_\infty \left(TI_{N2,j} - T_\infty \right) \tag{3.18}$$

And assuming the steady heat transfer in the reformer, the relationships between θ and T can be expressed as follows;

$$\theta_{1,j+1} = T_{1,j} + \frac{\alpha^i_{2,j} \cdot A^i_{2,j}}{2G_{1,j} \cdot C_{1,j}} \left(T_{2,j} - T_{1,j} \right) \tag{3.19}$$

$$\begin{aligned} \theta_{2,j} = T_{3,j} &+ \frac{\alpha^i_{4,j} \cdot A^i_{4,j}}{2G_{3,j} \cdot C_{3,j}} \left(T_{4,j} - T_{3,j} \right) - \frac{\alpha^0_{2,j} \cdot A^0_{2,j}}{2G_{3,j} \cdot C_{3,j}} \left(T_{3,j} - T_{2,j} \right) \\ &- \frac{Q_{3,j}}{2G_{3,j} \cdot C_{3,j}} - \frac{\alpha_{c,j} \cdot A_{c,j}}{2G_{3,j} \cdot C_{3,j}} \left(T_{3,j} - T_{c,j} \right) \end{aligned} \tag{3.20}$$

$$\theta_{3,j+1} = T_{5,j} - \frac{\alpha_{r,j} \cdot A_{r,j}}{2G_{5,j} \cdot C_{5,j}} \left(T_{5,j} - TI_{1,j} \right) - \frac{\alpha^0_{4,j} \cdot A^0_{4,j}}{2G_{5,j} \cdot C_{5,j}} \left(T_{5,j} - T_{4,j} \right) \tag{3.21}$$

Boundary conditions; $$\theta_{2,1} = \theta_{1,1} \tag{3.22}$$

$$\theta_{2,N+1} = \theta_{2,in} \tag{3.23}$$

3.2.2 Reaction Rate Equations

In the numerical analysis for the reforming process of the natural gas which consists of many kinds of hydro carbon, following reaction equations are employed.

steam reforming reaction;

$$CH_4 + 2H_2O \xrightarrow{r1} CO_2 + 4H_2 \quad (3.24)$$

water-gas shift reaction;

$$CO + H_2O \xrightarrow{r2} CO_2 + H_2 \quad (3.25)$$

CO_2 reforming reaction;

$$CH_4 + CO_2 \xrightarrow{r3} 2CO + 2H_2 \quad (3.26)$$

$$\begin{aligned} C_nH_m + xH_2O \xrightarrow{r4} & aH_2 + bCO + cCH_4 + dCO_2 + eC_2H_6 + fC_2H_4 \\ & + gC_3H_8 + hC_3H_6 + iC_4H_{10} + (x/2)CO_2 \end{aligned} \quad (3.27)$$

$$C_4H_{10} \xrightarrow{r5} C_4H_8 + H_2 \quad (3.28)$$

$$C_4H_{10} \xrightarrow{r6} C_2H_6 + C_2H_4 \quad (3.29)$$

$$C_4H_{10} \xrightarrow{r7} C_3H_6 + CH_4 \quad (3.30)$$

$$C_4H_8 + H_2 \xrightarrow{r8} C_2H_6 + C_2H_4 \quad (3.31)$$

$$C_3H_8 \xrightarrow{r9} C_2H_4 + CH_4 \quad (3.32)$$

$$C_3H_8 \xrightarrow{r10} C_3H_6 + H_2 \quad (3.33)$$

$$C_3H_8 \xrightarrow{r11} C_2H_6 + (1/2)C_2H_4 \quad (3.34)$$

$$C_3H_6 + H_2 \xrightarrow{r12} C_2H_4 + CH_4 \quad (3.35)$$

$$C_2H_6 + H_2 \xrightarrow{r13} 2CH_4 \quad (3.36)$$

$$C_2H_4 + H_2 \xrightarrow{r14} C_2H_6 \quad (3.37)$$

$$C_2H_6 + 4H_2O \xrightarrow{r15} 2CO_2 + 7H_2 \quad (3.38)$$

Rate expressions are often simple functions of reactant concentrations with a characteristic rate constant k. It does, however, depend strongly on temperature. Svante Arrhenius described this behavior in 1899 on the basis of numerous experimental rate measurements (12). Arrhenius found that the rate constants varied as the negative exponential tendency of the reciprocal absolute temperature, that is, $k(T) = k_0 \exp(-E/RT)$. This relationship is now known as the Arrhenius equation. In the Arrhenius equation, the temperature dependence comes primarily from the exponential term, although the quantity k_0, referred to as the frequency factor, may have a weak temperature dependence, no more than some fractional power of T. The units of k_0 are the same as the units of the rate constant k, since the exponential term has no units. The temperature (T) is in absolute or Kelvin units. The key quantity in the Arrhenius equation is the activation energy E. The activation energy can be thought of as the amount of energy, which must be supplied to the reactants in order to get them to react with other. Since this is a positive energy quantity, the majority of reactions have k increasing with temperature.

Reaction rates, r, for each reaction are defined by the following equations.

$$r_1 = k_1 \exp(-E_1/R \cdot T) \cdot (P_{CH4} \cdot P_{H2O}^2 - P_{CO2} \cdot P_{H2}^4 / K_1) \quad (3.39)$$

$$r_2 = k_2 \exp(-E_2/R \cdot T) \cdot (P_{CO} \cdot P_{H2O} - P_{CO2} \cdot P_{H2} / K_2) \quad (3.40)$$

$$r_3 = k_3 \exp(-E_3/R \cdot T) \cdot (P_{CH4} \cdot P_{CO2} - P_{CO}^2 \cdot P_{H2}^2 / K_3) \quad (3.41)$$

$$r_4 = k_4 \exp(-E_4/R \cdot T) \cdot P_{CnHm} \quad (3.42)$$

$$r_5 = k_5 \exp\left(-E_5 / R \cdot T\right) \cdot P_{C4H10} \tag{3.43}$$

$$r_6 = k_6 \exp\left(-E_6 / R \cdot T\right) \cdot P_{C4H10} \tag{3.44}$$

$$r_7 = k_7 \exp\left(-E_7 / R \cdot T\right) \cdot P_{C4H10} \tag{3.45}$$

$$r_8 = k_8 \exp\left(-E_8 / R \cdot T\right) \cdot P_{C4H8} \tag{3.46}$$

$$r_9 = k_9 \exp\left(-E_9 / R \cdot T\right) \cdot P_{C3H8} \tag{3.47}$$

$$r_{10} = k_{10} \exp\left(-E_{10} / R \cdot T\right) \cdot P_{C3H8} \tag{3.48}$$

$$r_{11} = k_{11} \exp\left(-E_{11} / R \cdot T\right) \cdot P_{C3H8} \tag{3.49}$$

$$r_{12} = k_{12} \exp\left(-E_{12} / R \cdot T\right) \cdot P_{C3H6} \cdot P_{H2} \tag{3.50}$$

$$r_{13} = k_{13} \exp\left(-E_{13} / R \cdot T\right) \cdot P_{C2H6} \cdot P_{H2} \tag{3.51}$$

$$r_{14} = k_{14} \exp\left(-E_{14} / R \cdot T\right) \cdot P_{C2H4} \cdot P_{H2} \tag{3.52}$$

$$r_{15} = k_{15} \exp\left(-E_{15} / R \cdot T\right) \cdot P_{C2H6} \tag{3.53}$$

3.2.3 Mass Balance Equations

Mass balance equations for each component are as follows;

$$G_{H2,j} = G_{H2,j+1} + W(3r_1 + r_2 + 2r_3 + ar_4 + r_5 - r_8 + r_{10} - r_{13} - r_{14} + 7r_{15}) \tag{3.54}$$

$$G_{CO,j} = G_{CO,j+1} + W(-r_2 + 2r_3) \tag{3.55}$$

$$G_{CH4,j} = G_{CH4,j+1} + W(-r_1 - r_3 + br_4 + r_7 + r_9 + r_{12} + 2r_{13}) \tag{3.56}$$

$$G_{CO2,j} = G_{CO2,j+1} + W(r_1 + r_2 - r_3 + ir_4 + 2r_{15}) \tag{3.57}$$

$$G_{C2H6,j} = G_{C2H6,j+1} + W(dr_4 + r_6 + r_8 + r_{11} - r_{13} + r_{14} - r_{15}) \tag{3.58}$$

$$G_{C2H4,j} = G_{C2H4,j+1} + W(cr_4 + r_6 + r_8 + r_9 + 0.5r_{11} + r_{12} - r_{14}) \tag{3.59}$$

$$G_{C3H8,j} = G_{C3H8,j+1} + W(fr_4 - r_9 - r_{10} - r_{11}) \tag{3.60}$$

$$G_{C3H6,j} = G_{C3H6,j+1} + W(er_4 + r_7 + r_{10} - r_{12}) \tag{3.61}$$

$$G_{C4H10,j} = G_{C4H10,j+1} + W(hr_4 - r_5 - r_6 - r_7) \tag{3.62}$$

$$G_{C4H8,j} = G_{C4H8,j+1} + W(gr_4 + r_5 - r_8) \tag{3.63}$$

$$G_{CnHm,j} = G_{CnHm,j+1} - Wr_4 \tag{3.64}$$

$$G_{H2O,j} = G_{H2O,j+1} + W(-2r_1 - r_2 - xr_4 - 4r_{15}) \tag{3.65}$$

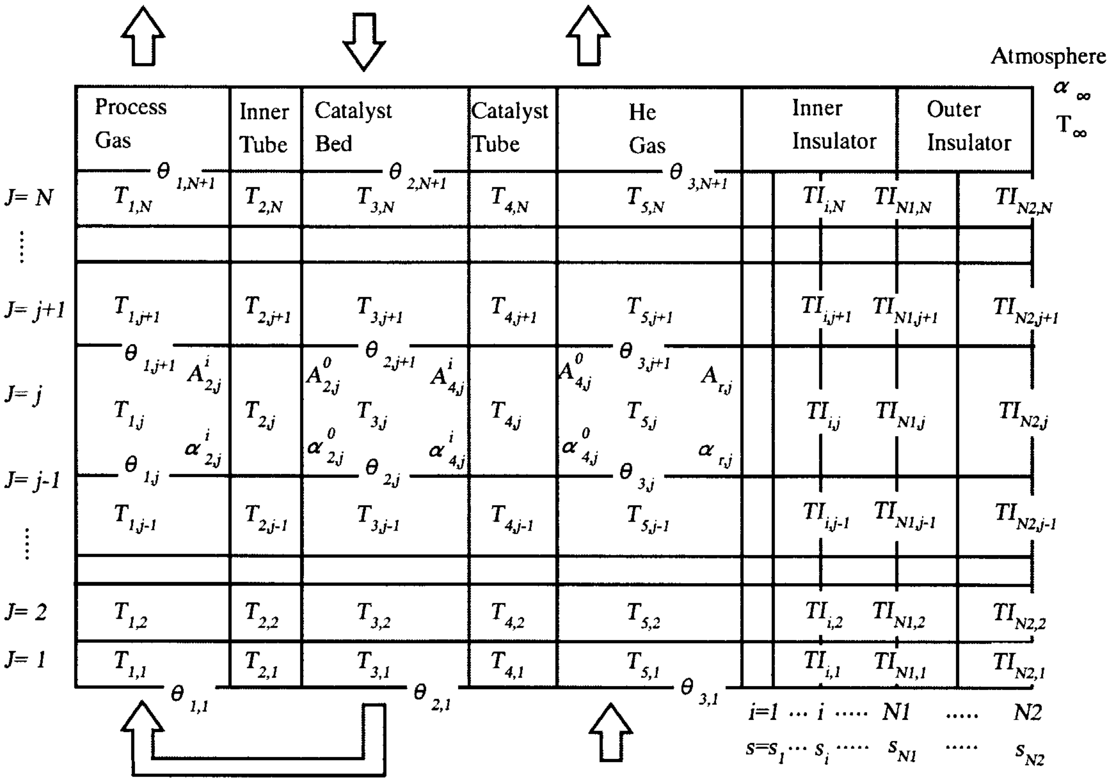

Fig.3.1 Variables allocated in cells

4. Numerical Analysis Results and Discussion of CO_2 Reforming

4.1 Standard Condition

The standard condition at reformer for CO_2 reforming is listed in Table 4.1, and molar ratio of CO_2 to CH_4 in the feed gas is 1.0. The heat and mass balance of the thermal and chemical process of the out-of-pile test facility under the standard operating condition was analyzed and the results are listed in Table 4.2. The heat and mass transfer are in a balanced condition, the process gas flow rate is G_1=0.0456kg/s, the helium flow rate is G_3=0.0911kg/s, and the heat power is Q_4=88.6k J/s.

Conversion ratio for the component i (ξ_i) is defined as follows:

$$\xi_i = (G_{i,\,feed} - G_{i,\,product}) \,/\, G_{i,\,feed} \tag{4.1}$$

The conversion ratio of CH_4 and CO_2 (ξ_{CH4} and ξ_{CO2}) are 0.360 and 0.507, respectively. These values are corresponding to the equilibrium one at 1085K and 4.3MPa. And the production rate of H_2 and CO are 1.4kmol/h (= 31 Nm^3/h) and 2.2kmol/h (=49 Nm^3/h), respectively. Therefore, the ratio of H_2 to CO in the product gas is 0.64.

4.2 Effect of Pressure

Figure 4.1 shows the effect of the average process gas pressure in the reformer on ξ_{CH4} and ξ_{CO2}, which are indicated by the solid lines in the figure. With the increase of the pressure, ξ_{CH4} and ξ_{CO2} decrease slightly. But the differences between the highest value and the lowest one are not so large. For example, the highest value of ξ_{CH4} is 0.35 at the pressure of 3.3MPa and the lowest is 0.33 at 4.3MPa. ξ_{CO2} is always higher than ξ_{CH4}, although a feed ratio of unity is used. In the water-gas shift reaction expressed by Eq.(3.25), the selectivity towards CO formation is always higher than the selectivity towards H_2. This phenomenon implies that, in addition to the main CO_2 reforming reaction, the revise water-gas shift reaction is also taking place.

4.3 Effect of Temperature

Figure 4.2 (a) and (b) show the effect of He temperature (T_{He}) on ξ_{CH4} and the CH_4 reaction rate, and on ξ_{CO2} and the CO_2 reaction rate, respectively. With the increase of T_{He}, ξ_{CH4} and ξ_{CO2} increase due to the increase of the CH_4 reaction rate and CO_2 reaction rate., respectively. The effect of T_{He} on the conversion ratio is higher than that of the pressure. With the increase of T_{He} from 1103 to 1253K, ξ_{CH4} increases from 0.28 to 0.52 by 1.9 times and ξ_{CO2} increases from 0.42 to 0.66 by 1.6 times, respectively.

4.4 Effect of CO_2/CH_4 ratio

Figure 4.3 (a) and (b) show the effect of CO_2/CH_4 ratio on ξ_{CH4} and the CH_4 reaction rate, and on ξ_{CO2} and the CO_2 reaction rate, respectively. In this analysis case, CO_2/CH_4 ratio was increased by the increase of the CO_2 flow rate, G_{CO2}, with the constant CH_4 flow rate, G_{CH4}= 2.7kmol/h. With the increase of CO_2/CH_4 ratio, the CH_4 reaction rate increases due to the increase of the forward reaction rate of CO_2 reforming expressed by Eq.(3.26) and results in the increase of ξ_{CH4}. And, with the increase of CO_2/CH_4 ratio, the CO_2 reaction rate increases, however, ξ_{CO2} decreases as shown in Fig.4.3(b). This is because the increase of G_{CO2} is higher than that of the CO_2 reaction rate. Therefore, ξ_{CO2} decreases.

Figure 4.3 (c) shows the effect of CO_2/CH_4 ratios on the production rate of H_2 and CO. With the increase of CO_2/CH_4 ratio, the production rate of CO increases. On the other hand, the production rate of H_2 takes almost constant value, about 1.4kmol/h. The forward reaction rate of CO_2 reforming increases with the increases of G_{CO2} and results in the increase of the production rate of H_2 and CO according to this reaction, however, produced H_2 reacts with CO_2 and synthesizes CO, according to the reverse water-gas shift reaction which increase with the increase of G_{CO2}. In these results, production rate of H_2 takes a constant value and that of CO increases. With the increase of CO_2/CH_4 ratio from 0.50 to 2.0, the sum of H_2 and the CO production rate shown by the broken line increases from 3.0 to 4.3, however, the ratio of the H_2 production rate to the CO (H_2/CO ratio) decreases from 0.82 to 0.46, respectively. H_2/CO ratio of 1.0 and 2.0 in the acetic acid and methanol formation process is required, respectively. Theses results indicate that the CO_2/CH_4 ratio should be decreased below 0.5 to obtain an H_2/CO ratio above 1.0 and the high CO_2/CH_4 ratio is desirable only for the CH_4 conversion ratio.

4.5 Effect of Activation Energy

Figure 4.4 shows the effect of the activation energy, E , for the CO_2 reforming reaction on ξ_{CH4} and ξ_{CO2} by the solid lines. With the increase of E from 75 to 130kJ/mol, ξ_{CH4} and ξ_{CO2} decrease from 0.36 to 0.25 and from 0.51 to 0.40, respectively. The reaction rate of CH_4 and CO_2 according to the CO_2 reforming reaction decreases with the increase of E . On the other hand, the reaction rate of CO_2 according to the water-gas shift reaction is independent on E . Therefore, ξ_{CH4} and ξ_{CO2} decrease and the decreasing tendency of ξ_{CO2} is same as that of ξ_{CH4}. If activation energy is high, which means the reaction rate is low, process gas flow rate should be decreased to obtain the high conversion ratio.

Table 4.1 Standard calculating conditions

		CO_2 reforming	CO_2 + H_2O reforming
He	Inlet temperature	1153K (= 880°C)	
	Exit pressure	4.1MPa	
Process gas	Inlet temperature	723K (= 450°C)	
	Inlet pressure	4.3MPa	
	CH_4 feed flow rate	0.012kg/s (= 2.7kmol/h)	
	CO_2 feed flow rate	0.033kg/s (= 2.7kmol/h)	0.011kg/s (= 0.9kmol/h)
	H_2O feed flow rate	—	0.009kg/s (= 1.8kmol/h)
	Molar ratio of CH_4:CO_2:H_2O	1 : 1 : 0	3 : 1 : 2

Table 4.2 Mass and heat balance of CO_2 reforming

Parameters	Value
(1) Reformer mass balance:	
Reactant gases flow rate, inlet to reformer. G1 [kg/s]:	0.0456
Product gases flow rate, outlet of reformer. G2 [kg/s]:	0.0456
Hot helium flow rate, inlet to reformer. G3 [kg/s]:	0.0911
Cold helium flow rate, outlet of reformer. G4 [kg/s]:	0.0911
(2) Reformer heat balance (temperature):	
Reactant gases temperature, inlet to reformer. T1 [K]:	741.2
Product gases temperature, outlet of reformer. T2 [K]:	883.1
Hot helium temperature, inlet to reformer. T3 [K]:	1153.1
Cold helium temperature, outlet of reformer. T4 [K]:	965.8
(3) Reformer heat balance (enthalpy):	
Reactant gases enthalpy, inlet to reformer. H1 [kJ/kg]:	975.4
Product gases enthalpy, outlet of reformer. H2 [kJ/kg]:	1454.3
Apparent heat absorbed by gases. Q1=G1 * (H2 -H1) [kJ]:	21.9
CH_4 flow rate inlet to reformer. G5 [kg/s]:	0.0120
Product gases flow rate outlet of reformer. G6[kg/s]:	0.0451
CH_4 composition in product gases. Y1 (wt. 100%):	0.170
CH_4 flow rate out of reformer. G7=G6 * Y1 [kg/s]:	0.00760
CH_4 conversion rate, ξ_{CH4}=(G5 - G7)/G5, (*100%):	0.363
ΔH for the reaction [kJ/mol]:	248.0
Chemical heat absorbed by gases. Q2=G5 * ξ_{CH4}/16 *1000 *E. [kJ/s]:	67.3
Total heat cost by gases. Q3=Q1 +Q2. [kJ/s]:	89.2
Hot helium enthalpy, inlet to reformer. H3 [kJ/kg]:	5984.7
Cold helium enthalpy, outlet of reformer. H4 [kJ/kg]:	5012.7
Heat transferred from helium, Q4=G3 * (H3 - H4), [kJ/s]:	88.6
Helium specific heat, Cp [J/(kg·K)]:	5198.0
Heat transferred from helium, Q5=Cp* G3 * (T3 -T4) [kJ/s]:	88.7

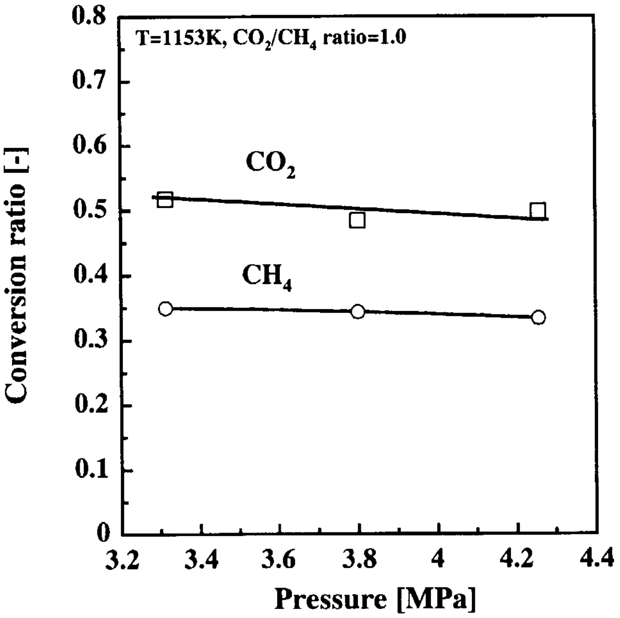

Fig.4.1 Effect of reformer pressure on conversion ratio of CO_2 reforming

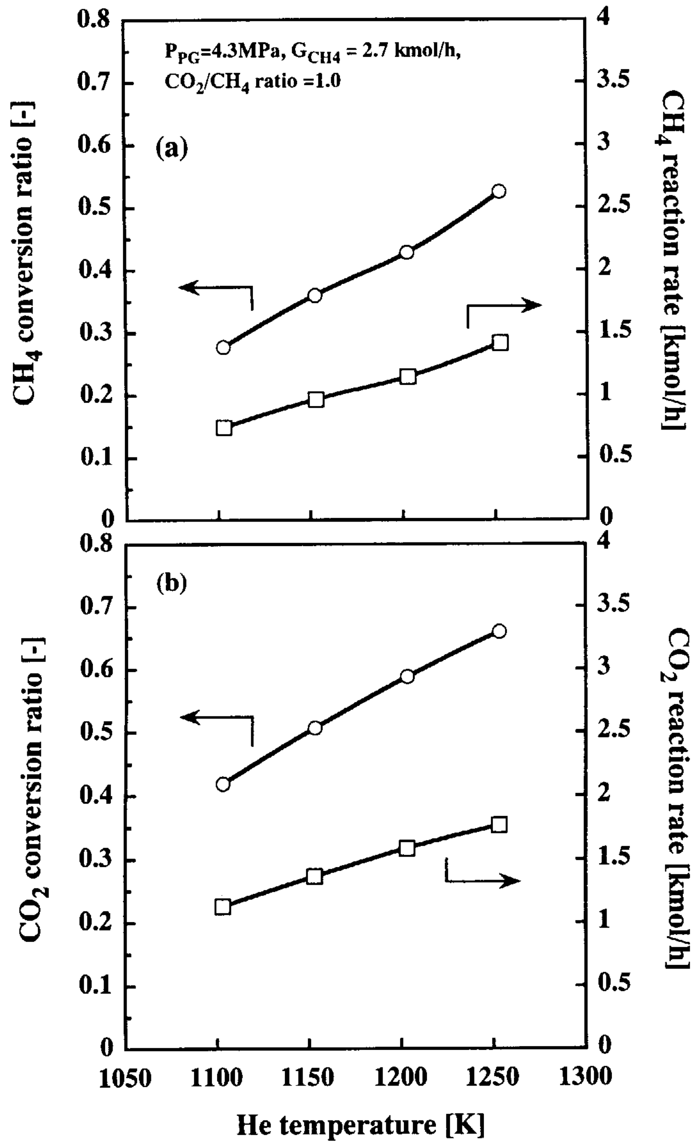

Fig.4.2 Effect of He temperature on conversion ratio and reaction rate of CO_2 reforming

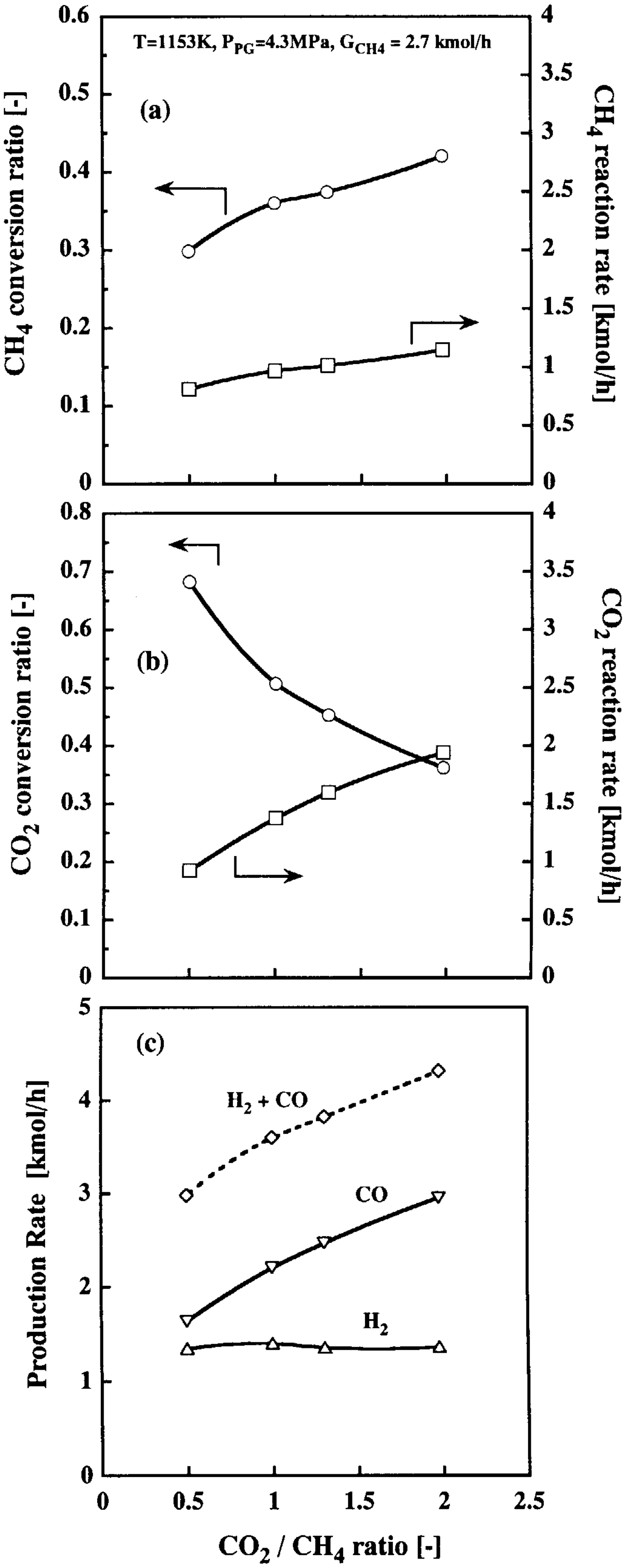

Fig.4.3 Effect of CO_2/CH_4 ratio on CO_2 reforming
(a) CH_4 conversion ratio and reaction rate: (b) CO_2 conversion ratio and reaction rate
(c) Production rate of H_2 and CO

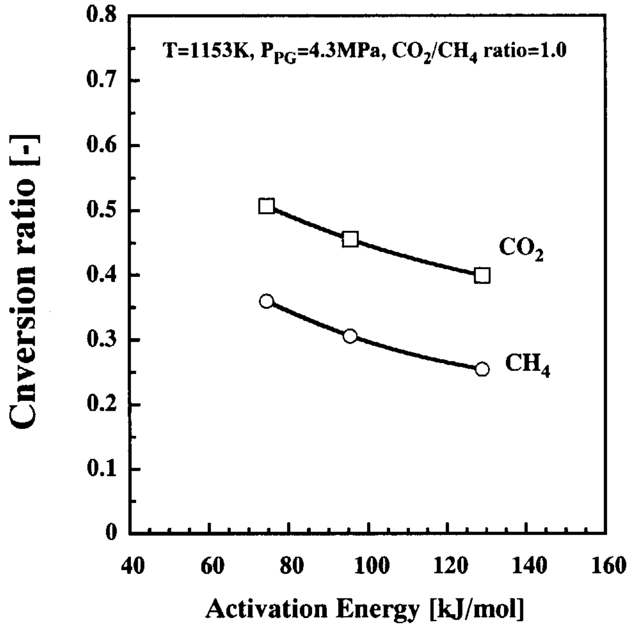

Fig.4.4 Effect of activation energy on conversion ratio of CO_2 reforming

5. Numerical Analysis Results and Discussion of CO_2+H_2O Reforming

5.1 Standard Condition

The standard condition at reformer for CO_2+H_2O reforming is also listed in Table 4.1. For the purpose is to obtain a gas product of which the molar ratio of H_2 to CO is 2, which is the best composition for methanol forming under the feed gas composition of CH_4:CO_2:H_2O = 3:1:2. Table 5.1 shows the heat and mass balance of CO_2+H_2O reforming under the standard operating condition and it confirms that mass and heat transfer are in a balanced condition. The results of the numerical analysis under the standard operating conditions are as follows;

ξ_{CH4}=0.35, ξ_{CO2}=0.397, ξ_{H2O}=0.347.

These values are corresponding to the equilibrium one at 1100K and 4.3MPa. And the production rate of H_2 and CO are 2.4kmol/h (= 54 Nm^3/h) and 1.3kmol/h (=28 Nm^3/h), respectively. Therefore, the ratio of H_2 to CO in the product gas is 1.9.

5.2 Effect of He Temperature

Figure 5.1 shows the effect of T_{He} on ξ_{CH4} and ξ_{CO2} by the solid lines. With the increase of T_{He} from 1153K to 1253K, ξ_{CH4} and ξ_{CO2} increase from 0.35 and 0.38 to 0.49 and 0.52, respectively. Comparing with the CO_2 reforming, ξ_{CH4} at each temperature reveals an almost equal value with the figures shown in fig4.1. On the other hand, ξ_{CO2} of the CO_2+H_2O reforming is lower than that of the CO_2 reforming. This is because CO_2 is not only consumed by the CO_2 reforming, but is also produced by the steam reforming in the CO_2+H_2O.

5.3 Effect of CO_2/CH_4 ratio

Figure 5.2 (a) and (b) show the effect of the CO_2/CH_4 ratio on ξ_{CH4} and the CH_4 reaction rate, and on ξ_{CO2} and the CO_2 reaction rate, respectively. In this analysis case, the CO_2/CH_4 ratio was increased by the increase of G_{CO2} with the constant G_{CH4} and G_{H2O}. With the increase of the CO_2/CH_4 ratio, the CH_4 reaction rate increases slightly due to the increase of the forward reaction of the CO_2 reforming, and results in the increase of ξ_{CH4}. On the other hand, with the increase of the CO_2/CH_4 ratio, ξ_{CO2} increases and takes a maximum value 0.42 at CO_2/CH_4 with a ratio that equals 0.6 and thereafter slightly decreases. The CO_2 reaction rate increases with the increase of the CO_2/CH_4 ratio as shown in the fig.5.2(b). The increase of the CO_2 reaction rate is slightly higher than that of G_{CO2} below the CO_2/CH_4 ratio of 0.6, however, above this point the increase of the CO_2 reaction rate which is restricted by the equilibrium becomes slightly lower than that of G_{CO2}. Therefore, ξ_{CO2} increases and then passes the maximum value and thereafter decreases.

Figure 5.2 (c) shows the effect of the CO_2/CH_4 ratio on the production rate of H_2 and CO. With the increase of the CO_2/CH_4 ratio, the production rate of H_2 and CO decreases and increases, respectively. Compared with the CO_2 reforming process, the production rate of H_2 for CO_2+H_2O reforming is higher than that for CO_2 due to the forward reaction of the steam reforming. In this analysis condition, the H_2/CO ratio is 2.0 at a CO_2/CH_4 ratio of 0.3 and 1.0 at a CO_2/CH_4 ratio of 1.0. Therefore, CO_2+H_2O reforming in the out-of-pile test facility is available for the production of synthesis gas of which the composition can be adjusted by the CO_2/CH_4 feed ratio.

5.4 Effect of H_2O/CH_4 ratio

Figure 5.3 (a) and (b) show the effect of the H_2O/CH_4 ratio on ξ_{CH4} and the CH_4 reaction rate, and on ξ_{CO2} and the CO_2 reaction rate, respectively. In this analysis case, the H_2O/CH_4 ratio was increased by the increase of G_{H2O} with the constant G_{CH4} and G_{CO2}. With the increases of the H_2O/CH_4 ratio, the CH_4 reaction rate increases and results in the increases of ξ_{CH4}. On the other hand, the CO_2 reaction rate decreases and becomes lower than 0 above a H_2O/CH_4 ratio of 1.45. This means that the CO_2 flow rate increases at the outlet of the reformer compared with that at the inlet. Therefore, the forward reaction rate of the water-gas shift reaction which produce CO_2 exceeds the forward reaction rate of the CO_2 reforming which consumes CO_2 , above a value of H_2O/CH_4 equaling 1.45.

Figure 5.3 (c) shows the effect of the H_2O/CH_4 ratio on the production rate of H_2 and CO. With the increase of the H_2O/CH_4 ratio, the production rate of H_2 and CO increases and slightly decreases, respectively. With the increase of H_2O/CH_4 ratio, that is the increase of G_{H2O}, the forward reaction rates of the steam reforming and the water-gas shift reactions increase. Therefore, the production rate of H_2 increases and that of CO decreases. The H_2/CO ratio increases from 1.76 to 4.43 with the increase of the H_2O/CH_4 ratio from 0.54 to 2.6. The production ratio of H_2/CO in which the ratio = 2.0, is the optimum condition for methanol production, and can be obtained in the condition of a feed ratio of $CH_4 : CO_2 : H_2O$ =3 : 1 : 2.1.

Table 5.1 Mass and heat balance of CO_2+H_2O reforming

Parameters	Value
(1) Reformer mass balance:	
Reactant gases flow rate, inlet to reformer. G1 [kg/s]:	0.0316
Product gases flow rate, outlet of reformer. G2 [kg/s]:	0.0316
Hot helium flow rate, inlet to reformer. G3 [kg/s]:	0.0911
Cold helium flow rate, outlet of reformer. G4 [kg/s]:	0.0911
(2) Reformer heat balance (temperature):	
Reactant gases temperature, inlet to reformer. T1 [K]:	854.3
Product gases temperature, outlet of reformer. T2 [K]:	934.6
Hot helium temperature, inlet to reformer. T3 [K]:	1153.1
Cold helium temperature, outlet of reformer. T4 [K]:	1008.5
(3) Reformer heat balance (enthalpy):	
Reactant gases enthalpy, inlet to reformer. H1 [kJ/kg]:	1962.6
Product gases enthalpy, outlet of reformer. H2 [kJ/kg]:	2263.6
Apparent heat absorbed by gases. Q1=G1 * (H2 -H1) [kJ]:	9.51
CH_4 flow rate inlet to reformer. G5 [kg/s]:	0.0120
Product gases flow rate outlet of reformer. G6[kg/s]:	0.0316
CH_4 composition in product gases. Y1 (wt. 100%):	0.247
CH_4 flow rate out of reformer. G7=G6 * Y1 [kg/s]:	0.00780
CH_4 conversion rate, ξ_{CH4}=(G5 - G7)/G5, (*100%):	0.350
ΔH for the reaction [kJ/mol]:	227.0
Chemical heat absorbed by gases. Q2=G5 * ξ_{CH4} /16 *1000 *E. [kJ/s]:	59.6
Total heat cost by gases. Q3=Q1 +Q2. [kJ/s]:	69.1
Hot helium enthalpy, inlet to reformer. H3 [kJ/kg]:	5984.8
Cold helium enthalpy, outlet of reformer. H4 [kJ/kg]:	5234.1
Heat transferred from helium, Q4=G3 * (H3 - H4), [kJ/s]:	68.4
Helium specific heat, Cp [J/(kg·K)]:	5198.0
Heat transferred from helium, Q5=Cp* G3 * (T3 -T4) [kJ/s]:	68.5

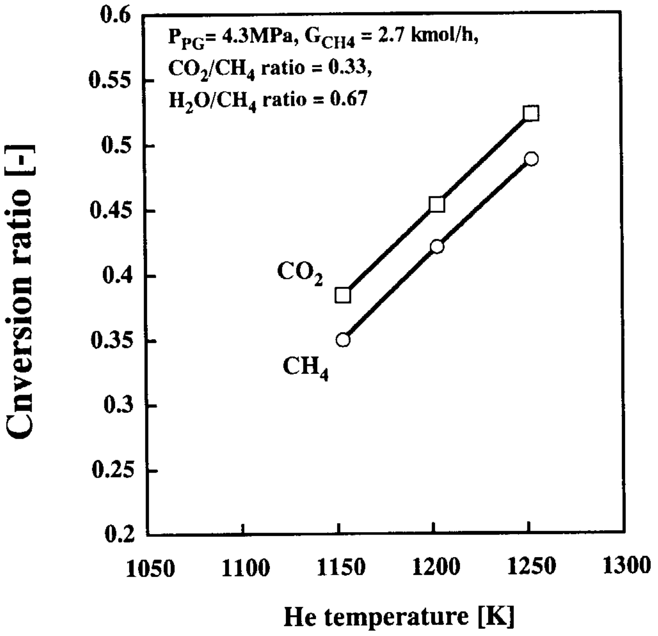

Fig.5.1 Effect of He temparature on conversion ratio of CO_2 + H_2O reforming

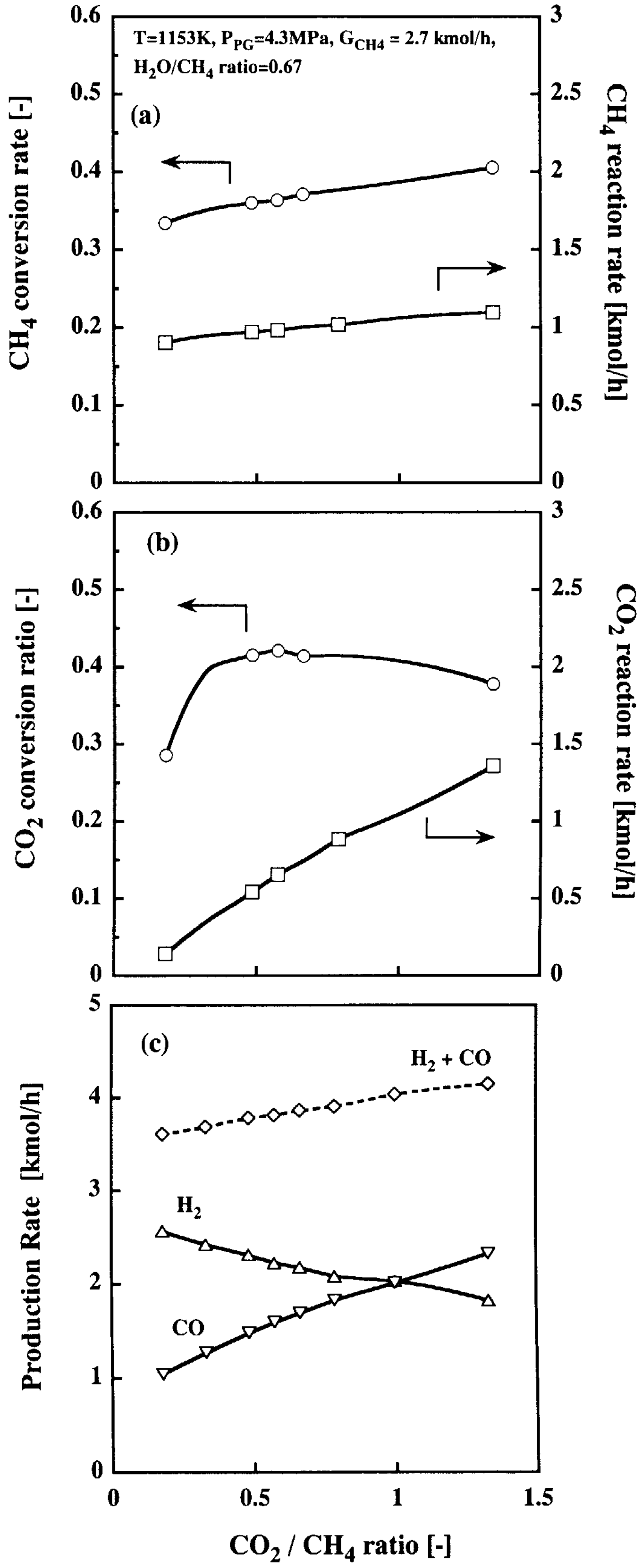

Fig.5.2 Effect of CO_2/CH_4 ratio on $CO_2 + H_2O$ reforming

(a) CH_4 conversion ratio and reaction rate: (b) CO_2 conversion ratio and reaction rate

(c) Production rate of H_2 and CO

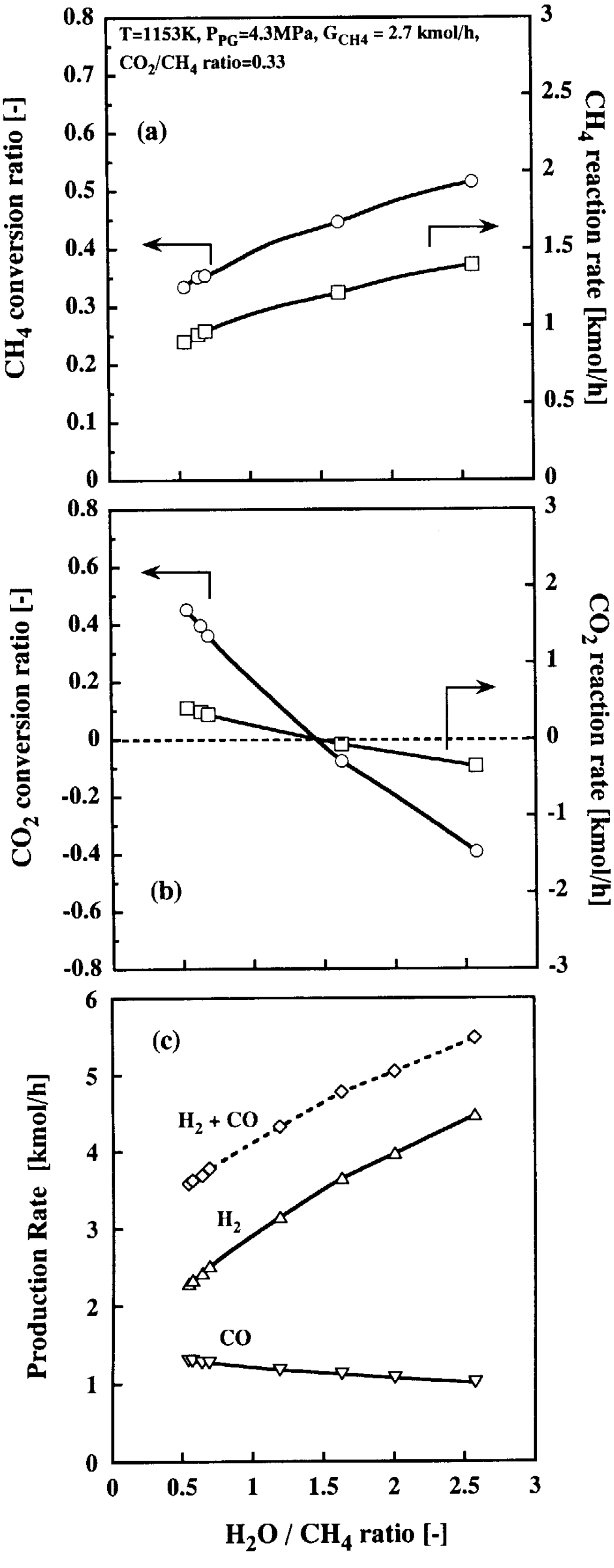

Fig.5.3 Effect of H_2O/CH_4 ratio on CO_2 + H_2O reforming

(a) CH_4 conversion ratio and reaction rate: (b) CO_2 conversion ratio and reaction rate

(c) Production rate of H_2 and CO

6. Concluding Remarks

(1) Significance

By means of its high coolant temperature, the HTGR reactor system offers various possibilities to use the resulting process heat economically. Establishment of a basic hydrogen production technology for the direct utilization of nuclear heat through the out-of-pile test facility of HTTR is of great significance for commercial process heat applications of HTGRs in the near future, and also to contribute the solution for the environmental issues regarding CO_2 emission. In order to check the feasibility of the CO_2 reforming in the out-of-pile test facility (which was originally designed for steam reforming) it appears a numerical simulation will need to be developed and evaluated in advance. With the numerical simulation of the CO_2 reforming in a catalytic reformer, it is relatively easy to assess the effect of various parameters and to estimate the extent of potential CO_2 usage.

(2) Conversion Ratio

From the numerical analysis of the CO_2 reforming and the CO_2+H_2O reforming, the CH_4 conversion ratio of 0.36 and 0.35 which correspond to the equilibrium one at 1085 and 1100K under the given standard calculating conditions (He temperature is 1153K) was obtained, respectively. The conversion of reactant gases depend significantly on the operating parameters such as the reforming temperature, which affects the thermodynamic equilibrium and reaction kinetics. The CH_4 conversion ratio increases with the increase of the helium temperature and the CO_2 flow rate, and the decrease of the catalyst activation energy.

The results show that tests of the CO_2 reforming and the CO_2+H_2O reforming can be carried out in the out-of-pile test facility without reconstruction of the facility.

(3) Preferable Conditions for Methane Reforming

The chemical reaction is restricted by the chemical equilibrium depending on both temperature and pressure. With a process gas reaction condition of 1073K and 4.2 MPa, the CH_4 conversion ratio in the steam reforming is nearly 0.60. There are three methods to improve the conversion ratio which are as follows;

(a) Increase of reaction temperature

If the reaction temperature increases up to 1223K, the CH_4 conversion ratio of steam reforming becomes about 0.90 in the reaction conditions of 4.5MPa and the feed flow ratio of steam to CH_4, S/C=3.5. In order to achieve this conversion ratio, He gas temperature at inlet of a reformer should be more than 1273K.

(b) Decrease of reaction pressure

If the reaction pressure decreases down to 1.0MPa, the CH_4 conversion ratio of steam reforming becomes about 0.90 in the reaction conditions of 1073K when S/C=3.5. Assuming a He gas pressure of 4.0MPa and a process gas pressure of 1.0MPa, the external pressure of 3.0MPa acts on a catalyst tube of the steam reformer which is a pressure boundary between He and process gases. As a result, the catalyst tube will collapse due to creep. In the design of the catalyst tube, it is desirable that the internal pressure at the process gas side is larger than the external one at the helium gas side because the metal tube is strong enough for internal pressure but is easily affected by external pressures in a high temperature atmosphere. As for the HTTR hydrogen production system, the catalyst tube is specially designed taking into account the condition of an internal pressure larger than an external pressure, meaning the process gas pressure is more than 4.2MPa. Therefore, high pressure is required because of the associated HTTR, and to compensate for this high pressure, an increase in temperature (the high temperature of helium) is required.

(c) Membrane reformer-removal of product gas

The possibility of incorporating selective solvents or membranes into a reformer opens great improvement possibilities, since selective removal of one of the products would shift the equilibrium and create more favorable thermodynamic conditions for the process. This kind of reformer has a membrane, which removes hydrogen along with the reaction. However, this kind of reformer is still at a research stage because a high performance membrane has not yet been developed for large hydrogen permeability and good durability in a high temperature atmosphere.

The methods mentioned above to improve the CH_4 conversion ratio are not practical yet. There is one method to keep CH_4 from being wasted, which is, the recycling of residual CH_4. The residual CH_4 in a product gas after reforming is recycled to the reformer with a gas separator for reuse as a raw material.

Acknowledgements

The authors would like to acknowledge the valuable discussions and comments provided by Dr. Hino, and want to express their gratitude to Dr. Ogawa for his continuous encouragement and support of the present study.

References

(1) J.Singh, H.F.Niessen, R.Harth, H.Fedders, H.Reutler, W.Panknin, W.D.Muller and H.G.Harms, The nuclear heated steam reformer – design and semitechnical operating experiences: Nuclear Engineering and Design, 78, 179 (1984)

(2) J.H.Edwards and A.M.Maitra, The reforming of methane with carbon dioxide – current status and future applications: Natural Gas Conversion Ⅱ, 291 (1994)

(3) R.Levitan, M.Levy, H.Rosin and R.Rubin, Closed-loop operation of a solar chemical heat pipe at the Weizmann Institute solar furnace: Solar Energy Materials 24, 464 (1991)

(4) O.Takayasu, C.Soman, Y.Takegahara, and I.Matsuura, Deactivation of Ni-catalyst and its prevention by mechanically mixing an oxide for the formation reaction of $CO+H_2$ from CO_2+CH_4: Catalyst Deactivation 1994 Studies in Surface Science and Catalysis, 88, 281 (1994)

(5) Z.L.Zhang, V.A.Tsipouriari, A.M.Efstathiou, and X.E.Verykios, Reforming of methane with carbon dioxide to synthesis gas over supported Rhodium catalysts- Ⅰ. Effects of support and metal crystallite size on reaction activity and deactivation characteristics: Journal of Catalysis, 158, 51 (1996).

(6) T.Inui, K.Saigo, Y.Fujii, K.Fujioka, Catalytic combustion of natural gas as the role of on-site heat supply in rapid catalytic CO_2-H_2O reforming of methane: Catalysis Today 26, 295 (1995)

(7) Z.Zhang, X.E.Verykios, Carbon dioxide reforming of methane to synthesis gas over Ni/La_2O_3 catalysts: Applied Catalysis A: General 138, 109 (1996)

(8) V.R.Choudhary, A.M.Rajput and B.Prabhakar, Energy efficient methane-to-syngas conversion with low H_2/CO ratio by simultaneous catalytic reactions of methane with carbon dioxide and oxygen: Catalysis Letters, 32, 391 (1995)

(9) K.Hada, T.Shibata, T.Nishihara and S.Shiozawa, Universally appliance design concept of stably controlling an HTGR-hydrogen production system: Journal of Japan Atomic Energy Society, 38, 834 (1996)

(10) Y.Inagaki, R.Hino, K.Hada, K.Haga, T.Nishihara, T.Takeda, and S.Shiozawa, Out-of-pile demonstration test program of HTTR hydrogen production system by steam reforming of natural, Proceedings of ICON 5: 5th International Conference on Nuclear Engineering 1997 France , ICONE5-2342, 1 (1997)

(11) Y.Inagaki, T.Nishihara, T.Takeda, K.Hada, M.Ogawa, S.Shiozawa, Y.Miyamoto, Development program on hydrogen production in HTTR: Seminar, IAEA 1998, held on November 2-5, in Beijing, China. 9 pages.

(12) M.V.Twigg, CATALYST HANDBOOK (second edition): Wolfe Publishing Ltd, 252 (1989)

Symbols

A :heat transfer area [m^2]
C :specific heat [J/(kg K)]
D :equivalent diameter [m]
e :internal energy [J/kg]
E :activation energy [J/mol]
f :friction factor [-]
F :force of friction per unit length [N/m]
g :gravitational acceleration [m/s^2]
G :gas flow rate [mol/s]
h :enthalpy [J/kg]
k :frequency factor [$mol/(m^3$ s Pa*)]
K :equilibrium coefficient [Pa**]
L :length of channel [m]
m_i :mass fraction of component i [-]
M_i :molecular weight of component i [-]
P :pressure [Pa]
Q :quantity of heat for the endothermic reaction [J/s]
Q_w :input thermal energy per unit volume [J/(s m^2)]
r :reaction rate per unit catalyst weight [mol/(kg·s)]
R :gas constant [J/(mol K)]
s :cell diameter of the heat insulater [m]
T :temperature of a cell [K]
TI :temperature of heat insulating material [K]
u :flow velocity [m/s]
W :catalyst weight [kg]
α :heat transfer coefficient [W/(m^2 K)]
ς :correction factor [-]
θ :temperature of a cell boundary [K]
λ :thermal conductivity [W/(m K)]
ρ :density [kg/m^3]

Superscripts
0 : internal wall
i : external wall

Subscripts
i :radial cell number of heat insulating (=1, 2 ,···, N1, ···, N2)
j :axial cell number (=1, 2 ,···, N)
1 :product gas
2 :inner tube
3 :reactant gas
4 :outer pipe
5 :He gas

国際単位系(SI)と換算表

表1　SI基本単位および補助単位

量	名称	記号
長さ	メートル	m
質量	キログラム	kg
時間	秒	s
電流	アンペア	A
熱力学温度	ケルビン	K
物質量	モル	mol
光度	カンデラ	cd
平面角	ラジアン	rad
立体角	ステラジアン	sr

表3　固有の名称をもつSI組立単位

量	名称	記号	他のSI単位による表現
周波数	ヘルツ	Hz	s^{-1}
力	ニュートン	N	$m\cdot kg/s^2$
圧力，応力	パスカル	Pa	N/m^2
エネルギー，仕事，熱量	ジュール	J	$N\cdot m$
工率，放射束	ワット	W	J/s
電気量，電荷	クーロン	C	$A\cdot s$
電位，電圧，起電力	ボルト	V	W/A
静電容量	ファラド	F	C/V
電気抵抗	オーム	Ω	V/A
コンダクタンス	ジーメンス	S	A/V
磁束	ウェーバ	Wb	$V\cdot s$
磁束密度	テスラ	T	Wb/m^2
インダクタンス	ヘンリー	H	Wb/A
セルシウス温度	セルシウス度	℃	
光束	ルーメン	lm	$cd\cdot sr$
照度	ルクス	lx	lm/m^2
放射能	ベクレル	Bq	s^{-1}
吸収線量	グレイ	Gy	J/kg
線量当量	シーベルト	Sv	J/kg

表2　SIと併用される単位

名称	記号
分，時，日	min，h，d
度，分，秒	°，′，″
リットル	l，L
トン	t
電子ボルト	eV
原子質量単位	u

$1\ \text{eV} = 1.60218\times10^{-19}\ \text{J}$

$1\ \text{u} = 1.66054\times10^{-27}\ \text{kg}$

表4　SIと共に暫定的に維持される単位

名称	記号
オングストローム	Å
バーン	b
バール	bar
ガル	Gal
キュリー	Ci
レントゲン	R
ラド	rad
レム	rem

$1\ \text{Å} = 0.1\ \text{nm} = 10^{-10}\ \text{m}$

$1\ \text{b} = 100\ \text{fm}^2 = 10^{-28}\ \text{m}^2$

$1\ \text{bar} = 0.1\ \text{MPa} = 10^5\ \text{Pa}$

$1\ \text{Gal} = 1\ \text{cm/s}^2 = 10^{-2}\ \text{m/s}^2$

$1\ \text{Ci} = 3.7\times10^{10}\ \text{Bq}$

$1\ \text{R} = 2.58\times10^{-4}\ \text{C/kg}$

$1\ \text{rad} = 1\ \text{cGy} = 10^{-2}\ \text{Gy}$

$1\ \text{rem} = 1\ \text{cSv} = 10^{-2}\ \text{Sv}$

表5　SI接頭語

倍数	接頭語	記号
10^{18}	エクサ	E
10^{15}	ペタ	P
10^{12}	テラ	T
10^{9}	ギガ	G
10^{6}	メガ	M
10^{3}	キロ	k
10^{2}	ヘクト	h
10^{1}	デカ	da
10^{-1}	デシ	d
10^{-2}	センチ	c
10^{-3}	ミリ	m
10^{-6}	マイクロ	μ
10^{-9}	ナノ	n
10^{-12}	ピコ	p
10^{-15}	フェムト	f
10^{-18}	アト	a

（注）

1. 表1　5は「国際単位系」第5版，国際度量衡局 1985年刊行による。ただし，1 eVおよび1 uの値はCODATAの1986年推奨値によった。
2. 表4には海里，ノット，アール，ヘクタールも含まれているが日常の単位なのでここでは省略した。
3. barは，JISでは流体の圧力を表わす場合に限り表2のカテゴリーに分類されている。
4. EC閣僚理事会指令ではbar，barnおよび「血圧の単位」mmHgを表2のカテゴリーに入れている。

換算表

力	$N(=10^5 dyn)$	kgf	lbf
	1	0.101972	0.224809
	9.80665	1	2.20462
	4.44822	0.453592	1

粘度　$1\ \text{Pa}\cdot\text{s}(\text{N}\cdot\text{s/m}^2) = 10\ \text{P}$(ポアズ)$(\text{g}/(\text{cm}\cdot\text{s}))$

動粘度　$1\ \text{m}^2/\text{s} = 10^4\ \text{St}$(ストークス)$(\text{cm}^2/\text{s})$

圧力	MPa(=10 bar)	kgf/cm^2	atm	mmHg(Torr)	lbf/in^2(psi)
	1	10.1972	9.86923	7.50062×10^3	145.038
	0.0980665	1	0.967841	735.559	14.2233
	0.101325	1.03323	1	760	14.6959
	1.33322×10^{-4}	1.35951×10^{-3}	1.31579×10^{-3}	1	1.93368×10^{-2}
	6.89476×10^{-3}	7.03070×10^{-2}	6.80460×10^{-2}	51.7149	1

エネルギー・仕事・熱量	$J(=10^7 erg)$	kgf・m	kW・h	cal(計量法)	Btu	ft・lbf	eV
	1	0.101972	2.77778×10^{-7}	0.238889	9.47813×10^{-4}	0.737562	6.24150×10^{18}
	9.80665	1	2.72407×10^{-6}	2.34270	9.29487×10^{-3}	7.23301	6.12082×10^{19}
	3.6×10^6	3.67098×10^5	1	8.59999×10^5	3412.13	2.65522×10^6	2.24694×10^{25}
	4.18605	0.426858	1.16279×10^{-6}	1	3.96759×10^{-3}	3.08747	2.61272×10^{19}
	1055.06	107.586	2.93072×10^{-4}	252.042	1	778.172	6.58515×10^{21}
	1.35582	0.138255	3.76616×10^{-7}	0.323890	1.28506×10^{-3}	1	8.46233×10^{18}
	1.60218×10^{-19}	1.63377×10^{-20}	4.45050×10^{-26}	3.82743×10^{-20}	1.51857×10^{-22}	1.18171×10^{-19}	1

1 cal = 4.18605 J（計量法）
= 4.184 J　（熱化学）
= 4.1855 J　(15 °C)
= 4.1868 J（国際蒸気表）

仕事率　1 PS（仏馬力）
= 75 kgf・m/s
= 735.499 W

放射能	Bq	Ci
	1	2.70270×10^{-11}
	3.7×10^{10}	1

吸収線量	Gy	rad
	1	100
	0.01	1

照射線量	C/kg	R
	1	3876
	2.58×10^{-4}	1

線量当量	Sv	rem
	1	100
	0.01	1

(86年12月26日現在)

THERMAL AND CHEMICAL ANALYSIS OF CARBON DIOXIDE REFORMING OF METHANE USING THE OUT-OF-PILE TEST FACILITY